Published in final edited form as:

*NMR Biomed*. 2021 January ; 34(1): e4419. doi:10.1002/nbm.4419.

# Oxidative Phosphorylation in Creatine Transporter Deficiency

**Shizhe Li**[1,§], **Simona Bianconi**[2,§], **Jan Willem van der Veen**[1], **An Dang Do**[2], **JoEllyn Stolinski**[3], **Kim M. Cecil**[4], **Fady Hannah-Shmouni**[2], **Forbes D. Porter**[2], **Jun Shen**[1,*]

[1]Molecular Imaging Branch, National Institute of Mental Health, Bethesda, MD, USA

[2]Division of Translational Medicine, *Eunice Kennedy Shriver* National Institute of Child Health and Human Development, Bethesda, MD, USA

[3]NMR Facility, National Institute of Neurological Disorders and Stroke, Bethesda, MD, USA

[4]Department of Radiology, Cincinnati Children's Hospital Medical Center and the University of Cincinnati College of Medicine, Cincinnati, Ohio, USA

## Abstract

X-linked creatine transporter deficiency (CTD) is one of the three types of the cerebral creatine deficiency disorders. CTD arises from pathogenic variants in the X-linked gene *SLC6A8*. We report the first phosphorus ($^{31}$P) MRS study of patients with CTD, where both phosphocreatine and total creatine concentrations were found to be markedly reduced. Despite the diminished role of creatine and phosphocreatine in oxidative phosphorylation in CTD, we found no elevation of lactate or lowered pH, indicating that the brain energy supply still largely relied on oxidative metabolism. Our results suggest that mitochondrial function is a potential therapeutic target for CTD.

### Keywords

$^{1}$H MRS; $^{31}$P MRS; Creatine; Creatine transporter deficiency

## INTRODUCTION

Creatine and its phosphorylated form play a central role in the energy metabolism in nervous tissue.[1] In particular, creatine and phosphocreatine (PCr) are coupled to the rapid exchanges between adenosine diphosphate (ADP) and adenosine triphosphate (ATP); the latter is the energy currency of all cells. Consequently, creatine is considered essential for proper brain development and function. Creatine is primarily synthesized in kidneys and liver by arginine:glycine amidinotransferase (AGAT) and guanidinoacetate methyltransferase (GAMT).[2] The enzymatic action of AGAT produces guanidinoacetate as a substrate for the production of creatine by GAMT. Creatine passes the blood brain barrier via the creatine

[*]**Address correspondence to:** Jun Shen, Ph.D., Molecular Imaging Branch, National Institute of Mental Health, Bldg. 10, Rm. 2D51A, 9000 Rockville Pike, Bethesda, MD 20892-1527, Tel.: (301) 451-3408, Fax: (301) 480-2397, shenj@mail.nih.gov.
[§]These authors contributed equally.

transporter to support energy metabolism in the brain.[3] Creatine is finally converted to creatinine through a spontaneous process and excreted in urine.[4]

Cerebral creatine deficiency disorders are rare inherited metabolic conditions in which the formation or transport of creatine is disrupted. Among children with intellectual disabilities of unknown origin, about 1–2% may have creatine deficiency.[5] Symptoms include but are not limited to developmental, speech and language delay, movement disorders, hypotonia, feeding intolerances, hyperactivity, seizures, and autistic-like behaviors.[5] Three types of cerebral creatine deficiency disorders exist: (a) AGAT deficiency (OMIM 612718; *GATM*, 15q21.1), (b) GAMT deficiency (OMIM 612736; *GAMT*, 19p13.3) and (c) creatine transporter deficiency (CTD, OMIM 300352; *SLC6A8*, Xq28). The first two are recessive disorders of creatine synthesis, while the third, CTD, is caused by pathogenic variants in the X-linked gene *SLC6A8*. These variants in *SLC6A8* are thought to affect transport of creatine and its precursors across the blood-brain barrier and amongst the different cell types in the brain.[6] Patients with AGAT or GAMT deficiency can be effectively treated by oral creatine supplementation.[7] In contrast, most patients with CTD respond poorly to creatine supplementation because of the blockade of creatine transport into brain cells.[5]

Creatine deficiency in the brain was first revealed by MRS in 1994.[8] Both proton ($^{1}$H) and phosphorus ($^{31}$P) MRS have become important tools for clinical study of AGAT and GAMT deficiency, including monitoring of their treatment with oral creatine supplementation. In general, these studies have found that the signals of total creatine (tCr = creatine plus PCr) and PCr of patients with AGAT and GAMT deficiency were greatly decreased.[7–10] After treatment with oral creatine supplementation, increases in the total creatine signal in $^{1}$H spectra and the PCr signal in $^{31}$P spectra were observed, accompanied by significant improvement in symptoms.[7–10]

CTD was first reported in 2001.[11,12] Subsequent $^{1}$H MRS studies demonstrated prominent reduction of the total creatine signal in $^{1}$H spectra.[11,13,14] To date, however, $^{31}$P MRS, which is a powerful tool for studying brain energy metabolism, has not been applied to CTD. Measuring phosphate-containing brain metabolites by $^{31}$P MRS is clearly of interest for understanding CTD and its treatments, as ample evidence has indicated the pivotal role of PCr and other phosphorus-containing metabolites in tissue's response to energy demand.[15,16] In this study, we sought to examine brain energetics under abnormally low total creatine levels using $^{31}$P MRS and $^{1}$H MRS in male patients with CTD.

## METHODS

### Participants

Fourteen male patients with CTD (mean age = 7.4 years; range 3 to 14 years) were recruited from the National Institutes of Health under protocol: 'Observational Study of Males with Creatine Transporter Deficiency (Vigilan), ClinicalTrials.gov Identifier: NCT02931682'. CTD diagnosis was confirmed by ascertaining a pathogenic variant in *SLC6A8* through direct sequencing, as well as biochemical confirmation of elevated creatine to creatinine ratio in urine. All patients with CTD were under propofol anesthesia during $^{1}$H and $^{31}$P MRS scans.

## MR procedures

*In vivo* $^{1}$H and $^{31}$P MRS scans were performed on a Siemens Skyra 3 T scanner (Siemens Healthcare, Erlangen, Germany). After the patient was placed in the magnet, $^{31}$P MRS was performed first, followed by $^{1}$H MRS. $^{31}$P Spectra were obtained using a custom-built RF coil assembly consisted of a circular $^{31}$P surface coil (inner diameter = 7.5 cm) and a $^{1}$H half-volume coil. The proton coil was mounted on a semi-cylindrical plastic tube (outer diameter = 20.3 cm) and consisted of two overlapped octagonal loops (length and width = 12.7 cm). The coil assembly was connected to the 3 T scanner via two interface boxes (Stark Contrast MRI Coils Research, Erlangen, Germany), one for the $^{1}$H coil and the other for the $^{31}$P coil. The boxes contained transmit-receive switches, pre-amplifiers and RF filters. After $^{31}$P spectra were obtained, a Siemens 20-channel $^{1}$H volume head coil (inner diameter = 22.9 cm and length = 25.4 cm) was used to acquire $^{1}$H MRS data.

A gradient echo based three-plane localizer was used to properly position the patient. Static magnetic ($B_0$) field shimming was performed using the Siemens 3D shim tool that includes full first- and second-order shimming. A voxel of 4 × 4 × 4 cm$^3$ located right above the $^{31}$P coil was selected to perform $B_0$ shimming in the occipital lobe (see Figure 1). To evaluate shimming results, a point resolved spectroscopy (PRESS) sequence was used to acquire a water spectrum from the shim voxel.

## $^{31}$P MRS

$^{31}$P spectra were acquired using a Siemens FID sequence with hard pulse length = 500 μs, SW = 5 kHz, number of data points = 1024, repetition time ($T_R$) = 2 s, and number of averages (NA) = 128. Fully relaxed $^{31}$P spectra ($T_R$ = 25 s and NA = 64) were also acquired for seven patients with CTD in addition to the scans with $T_R$ = 2 s. No $^{1}$H decoupling was applied. To avoid uneven distortion of $^{31}$P signal intensities, no nuclear Overhauser enhancement irradiation was applied.

## $^{1}$H MRS

$B_0$ field shimming for $^{1}$H MRS was performed using a Siemens 3D shim tool in the same 4 × 4 × 4 cm$^3$ voxel as that selected for $^{31}$P MRS. $^{1}$H spectra were acquired with a PRESS sequence. The RF excitation pulse was a Sinc-Gauss pulse and the refocusing pulses were an optimized selective 180$^o$ pulse. $T_R$ = 2 s, spectral width = 2 kHz, number of data points = 2048, NA = 128. The spectra were acquired from a single voxel of 2 × 2 × 2 cm$^3$ at the center of the shim voxel (see Figure 1). For each patient, $^{1}$H MRS spectra were acquired at echo time ($T_E$)= 30 ms and 135 ms.

## Postprocessing

The $^{31}$P data were read into a customized program, written in IDL (Harris Geospatial Solutions, Boulder, CO, USA), to set the first two complex points of the FIDs with $T_R$ = 2 s and the first three complex points of the FIDs with $T_R$ = 25 s to zeroes, in order to reduce strong and broad baseline signals. The frequency offset of phosphocreatine (PCr) was set to zero ppm and the spectra were zero and first order phase corrected. The $^{31}$P data were processed using jMRUI and fitted with the AMARES algorithm[17] using prior spectral knowledge of $^{31}$P metabolites.[17,18] The $^{31}$P basis set consisted of β-ATP, nicotinamide

adenine dinucleotide (NAD), α-ATP, γ-ATP, PCr, membrane phospholipids (MPs), glycerophosphocholine (GPC), glycerophosphoethanolamine (GPE), intracellular inorganic phosphate ($P_i^{in}$), extracellular inorganic phosphate ($P_i^{ex}$), phosphocholine (PC), phosphoethanolamine (PE) and uridine diphosphate glucose (UDPG). The $^1$H spectra were fitted using LCModel 6.3–1J with the standard basis sets for the echo times of 30 ms and 135 ms.

Following earlier studies of cerebral creatine deficiencies, the metabolites measured by proton MRS were expressed as ratios to N-acetylaspartate (NAA).[13,14] Total creatine, total choline (tCho), glutamate (Glu), myo-Inositol (mI) and lactate (Lac) were obtained from LCModel fitting of the $^1$H MRS data acquired at TE = 30 ms. Lactate was also extracted from the $^1$H MRS data acquired at $T_E$ = 135 ms, which is the optimal echo time for analyzing the lactate methyl doublet. $^{31}$P-containing metabolites including PCr, ATP, $P_i^{in}$, $P_i^{ex}$, NAD were fitted using jMRUI from the $^{31}$P MRS data acquired at $T_R$ = 2 s (n = 14) and 25 s (n = 7). Uridine diphosphate glucose (UDPG) was extracted from $^{31}$P spectra with $T_R$ = 25 s. $^{31}$P metabolite ratios such as total $P_i$ ($tP_i = P_i^{in} + P_i^{ex}$)/PCr, PCr/γ-ATP and UDPG/NAD were also calculated. Intracellular and extracellular pH values as indicated by the difference in chemical shift between inorganic phosphate and PCr were measured.

## RESULTS

### Metabolites by $^1$H MRS

Typical water linewidth (full width at half maximum) from the 64 cm$^3$ cubical shim voxel was 11–13 Hz. Echoing previous findings using proton MRS,[11,13,14] $^1$H spectra from patients with CTD show that total creatine was markedly reduced as evidenced by the weak creatine signal at $T_E$ = 30 ms (Figure 2a) and $T_E$ = 135 ms (Figure 2b). The linewidth and signal-to-noise (SNR) of NAA were found to be 5.1 ± 0.5 Hz and 55 ± 5, respectively. The average total creatine/NAA ratio was 0.12 ± 0.02 (n = 14; Table 1). In comparison, the total creatine/NAA ratio of healthy subjects reported in the literature is in the range of 0.65–0.81.[19–23] The lactate/NAA ratio of patients with CTD measured at $T_E$ = 30 and 135 ms was 0.042 ± 0.007 (n = 14) and 0.025 ± 0.014 (n = 14), respectively (Table 1). This is in line with the normal lactate level in the resting brain of healthy subjects found in other studies.[19,22,23]

Ratios of the other major metabolites detected by proton MRS, the Glu/NAA, Cho/NAA, and mI/NAA, were found to be 0.92 ± 0.14, 0.10 ± 0.01 and 0.51 ± 0.05 (n = 14), respectively, in patients with CTD, which are in agreement with the corresponding ratios of healthy subjects found in the literature (Table 1).

### Metabolites and pH by $^{31}$P MRS

Typical $^{31}$P spectra acquired from a patient with CTD at $T_R$ = 2 s and 25 s are shown in Figure 3a and 3b, respectively, these were scaled according to their number of signal averages. Resonances of PE, PC, $P_i^{ex}$, $P_i^{in}$, phosphodiester (PDE = GPE +GPC) + MP, PCr, NAD, and γ-, α-, and β-ATP were observed. To the best of our knowledge, this is the first report of *in vivo* measurement of brain $^{31}$P spectra of patients with CTD. The key feature of the $^{31}$P spectra is that the signal intensity of PCr was significantly reduced relative to healthy

subjects. The doublets of γ- and α-ATP, and the NAD, PE, PC, and $P_i^{ex}$ signals were clearly resolved even without proton decoupling. The linewidth and SNR of PCr were found to be 5.4 ± 0.5 Hz and 24 ± 4, respectively. The PCr/γ-ATP, $tP_i$/γ-ATP, $tP_i$/PCr, NAD/γ-ATP, UDPG/γ-ATP, and UDPG/NAD ratios were summarized in Table 2 for $T_R$ = 2 s and 25 s, respectively. The corresponding ratios of healthy subjects obtained from the literature were also given in Table 2.[24–33]

UDPG is the immediate precursor of glycogen, the latter stores glucose for energy metabolism in brain.[34] The $P_\beta$ peak of UDPG resonating at – 9.83 ppm was detected in the spectrum with $T_R$ = 25 s (Figure 3b). The UDPG signal was not clearly observed in the data acquired at $T_R$ = 2 s likely due to the long $T_1$ of UDPG.[29] Figure 4 shows the result of summing the seven patients' spectra with $T_R$ = 25 s, which reveals the $P_\beta$ peak of UDPG at – 9.83 ppm. The UDPG/NAD ratio of the patients with CTD was found to be 0.51 ± 0.16 (n = 7) at $T_R$ = 25 s. Our result is comparable to the UDPG/NAD ratio of healthy volunteers (0.28–0.88) reported in the literature.[29,31–33] A representative individual spectrum showing spectral fitting of UDPG by jMRUI is provided in the supplementary material.

From the in vivo $^{31}$P spectra, the pH values of patients with CTD were also measured using the chemical shift difference between $P_i$ and PCr. The intracellular pH of patients with CTD was found to be 7.06 ± 0.02 (n = 14), which is in line with previous measurements from healthy subjects and patients with cerebral creatine deficiencies due to enzyme defects.[7] The extracellular pH was found to be 7.51 ± 0.06 (n = 14), which is also in agreement with normal brain values.

### Oxidative phosphorylation

PCr is converted to creatine (Cr) by creatine kinase in response to increased energy demand.[35–37] In patients with CTD, the $tP_i$/PCr ratio was found to be 2.7 ± 0.5 ($T_R$ = 2 s, n = 14) and 2.8 ± 0.4 ($T_R$ = 25 s, n = 7). In comparison, for healthy subjects, the $tP_i$/PCr ratio reported in the literature is 0.26–0.44. As shown in Table 2, there was also a similarly striking difference in PCr/γ-ATP ratio between patients with CTD (from 0.22 ± 0.03 ($T_R$ = 2 s, n = 14) to 0.26 ± 0.03 ($T_R$ = 25 s, n = 7)) and healthy subjects (1.02–1.48).

## DISCUSSION

This study demonstrates that the PCr signal in the $^{31}$P spectra of patients with CTD is significantly reduced, which echoes the large reductions in total creatine observed in previous $^1$H MRS studies.[11,13,14] Since CTD was first identified in 2001,[11] $^1$H MRS has been used to detect reductions in total creatine in CTD. Because CTD is a rare disease, studies performed to date have been limited to a few participants. This study measured $^{31}$P and $^1$H MRS in 14 male patients with CTD, the largest cohort to date. This has allowed us to perform robust quantitative analyses of the observed metabolic changes and compare them to literature data.

Abnormal NAA levels have not been reported in patients with CTD. This is also supported by our proton MRS data which shows that the metabolite/NAA ratios are all within the normal range except for Cr/NAA (Table 1). With oral creatine supplementation, treatment of

patients with cerebral creatine deficiencies arising from enzymatic defects did not change NAA levels.[7,9] The tCr/NAA ratio measured in the current study is in agreement with earlier proton MRS studies of CTD.[13] As observed in the earlier studies of patients with CTD, the total creatine/NAA ratio in our patient group is also markedly below those of normal brain (Table 1).

Detection of a small amount of lactate using short $T_E$ $^1$H MRS ($T_E$ = 30 ms) is known to be unreliable due to spectral overlapping by macromolecules and potential contamination by scalp lipid signals. We further acquired $^1$H MRS spectra at $T_E$ = 135 ms from patients with CTD to minimize macromolecular contribution to the spectra. At $T_E$ = 135 ms, the signal of lactate methyl $^1$H doublet at 1.3 ppm is inverted by evolution of its scalar coupling to the α-proton of lactate.[38] Overall, we detected no significant increase in lactate at either $T_E$ = 30 ms or $T_E$ = 135 ms (Table 1). As elevated lactate is a marker of increased glycolytic activities,[39] a lack of significant elevation of lactate in CTD suggests that brain energy production remains dominated by oxidative metabolism in the presence of severe shortage of creatine and PCr. This conclusion is corroborated by the observation of normal intracellular pH in the brain of patients with CTD, as increased lactate production is strongly correlated with tissue acidosis.

UDPG is well-known as the immediate precursor of glycogen. Although brain does not have a very significant reserve of glycogen, its importance in meeting the energy demand of neuronal activities has been clearly recognized.[40] UDPG was recently detected using $^{31}$P MRS at 7 Tesla in the human brain *in* vivo.[29,31–33] Figure 4 represents, to the best of our knowledge, the first *in vivo* detection of UDPG at 3 Tesla. As shown by Table 2, the UDPG level of the CTD patients is within the range of healthy subjects reported in the literature[29,31–33] despite the large reduction in Cr and PCr.

The phospholipid signal, commonly referred to as MP, overlaps with phosphoesters at low magnetic fields.[25, 41] Without proton decoupling, free phosphoesters are often overestimated at low magnetic fields due to difficulties in reliably modeling the asymmetrical MP signal without proton decoupling.[25] Therefore, the phosphomonoester (PME = PE + PC) and PDE results were not listed in Table 2. As the reported values of PME and PDE in normal brain span a very large range,[25,26,42] it is difficult to detect any potential abnormalities in phosphoesters and corresponding cell membrane metabolism in patients with CTD at 3 Tesla.

Cr and PCr are considered essential in brain energy metabolism. The large amount of PCr in normal brain is thought to be necessary to act as an effective, mobilizable reservoir of high-energy phosphates to recycle ATP. Consistent with the overall reduction in total creatine, we found a largely reduced PCr signal in $^{31}$P MRS spectra of patients with CTD. A large reduction in PCr was also observed in untreated patients with AGAT and GAMT deficiencies. With oral creatine supplementation (and diet restriction in the case of GAMT deficiency to reduce concomitant overproduction of guanidinoacetate), PCr gradually returns to normal or close to normal levels accompanied by significant clinical improvement.[7–9] The treatment of AGAT and GAMT deficiencies requires lifelong ingestion of creatine as the human body normally consumes about 2–3 g of creatine per day, while most patients with

CTD are not effectively treated with creatine supplementation. Even with AGAT and GAMT deficiencies, there are concerns regarding the adverse effects associated with long-term creatine oral supplementation.[43] Therefore, exploration of alternative treatment strategies for cerebral creatine deficiencies may be necessary. A recent preclinical study of *SLC6A8* knockout mice has showed the benefit of using chemically modified creatine to facilitate creatine transport.[44] Proteomic studies of animal models of creatine transporter deficiency have also found structural abnormalities in mitochondria, supporting targeting mitochondrial function for CTD.[45] Both our $^{1}$H and $^{31}$P MRS results indicate that under very low availability of creatine and PCr, oxidative phosphorylation remains the primary venue to support brain energy metabolism. The markedly reduced PCr is consistent with altered mitochondrial function. Therefore, enhancing mitochondrial function[46] may be beneficial for patients with CTD.

In summary, the lack of significant lactate elevation, normal intra- and extracellular pH values, and a large reduction in PCr observed in patients with CTD suggest that energy production under severely impaired creatine transport remains dominated by oxidative metabolism. As oral creatine supplementation lacks efficacy for treating CTD, our results point to alternative treatment strategies, for example, by enhancing brain mitochondrial function.

## CONCLUSION

This study was the first to apply phosphorus MRS to CTD. As expected, both total creatine in $^{1}$H spectra and PCr in $^{31}$P spectra were significantly reduced in patients with CTD. Total creatine reduction in $^{1}$H MRS was consistent with previously published findings. The large reduction in PCr, normal pH and no significant elevation in lactate in CTD all point to domination by oxidative phosphorylation in brain energy metabolism despite the markedly reduced role played by creatine and PCr. The significant presence of UDPG found in patients with CTD here strongly suggests that the glycogenolytic pathway[47,48] is highly active to support oxidative metabolism while the role of PCr is diminished. Since an effective treatment has not been found for CTD, our results suggest that exploring brain mitochondrial function augmentation by repurposing existing metabolic enhancers may be warranted.

## Supplementary Material

Refer to Web version on PubMed Central for supplementary material.

## ACKNOWLEDGMENTS

The authors gratefully acknowledge the patients, parents and guardians who participated in the study. The authors thank Mr John Perreault, CRNP, for providing medical support, Ms Ioline Henter for excellent editorial assistance, and Lumos Pharma, LLC for sponsoring the Vigilan Trial. This work is supported by the Intramural Research Programs of NIMH, NICHD, NCATS, and NINDS.

## ABBREVIATIONS

| | |
|---|---|
| **AGAT** | arginine:glycine amidinotransferase |

| | |
|---|---|
| **ATP** | adenosine triphosphate |
| **Cho** | choline |
| **CTD** | creatine transporter deficiency |
| **GAMT** | guanidinoacetate methyltransferase |
| **Glu** | glutamate |
| **GPC** | glycerophosphocholine |
| **GPE** | glycerophosphoethanolamine |
| **Lac** | lactate |
| **mI** | myo-inositol |
| **MP** | membrane phospholipids |
| **NAA** | N-acetylaspartic acid |
| **NAD** | adenine dinucleotide |
| **PC** | phosphocholine |
| **PCr** | phosphocreatine |
| **PDE** | phosphodiester |
| **PE** | phosphoethanolamine |
| **$P_i^{ex}$** | extracellular inorganic phosphate |
| **$P_i^{in}$** | intracellular inorganic phosphate |
| **PME** | phosphomonoester |
| **PRESS** | point resolved spectroscopy |
| **SD** | standard deviation |
| **SNR** | signal-to-noise |
| **$tP_i$** | total inorganic phosphate ($P_i^{in}$ +$P_i^{ex}$) |
| **UDPG** | uridine diphosphate glucose |

## REFERENCES

1. Andres RH, Ducray AD, Schlattner U, Wallimann T, Widmer HR. Functions and effects of creatine in the central nervous system. Brain Res Bull. 2008;76(4):329–343. [PubMed: 18502307]
2. Brosnan JT, da Silva RP, Brosnan ME. The metabolic burden of creatine synthesis. Amino Acids. 2011;40(5):1325–1331. [PubMed: 21387089]
3. Christie DL. Functional insights into the creatine transporter. Subcell Biochem. 2007;46:99–118. [PubMed: 18652074]

4. Brosnan JT, Brosnan ME. Creatine metabolism and the urea cycle. Mol Genet Metab. 2010;100:S49–S52. [PubMed: 20304692]
5. Clark JF, Cecil KM. Diagnostic methods and recommendations for the cerebral creatine deficiency syndromes. Pediatr Res. 2015;77(3):398–405. [PubMed: 25521922]
6. Comeaux MS, Wang J, Wang G, et al. Biochemical, molecular, and clinical diagnoses of patients with cerebral creatine deficiency syndromes. Mol Genet Metab. 2013;109(3):260–268. [PubMed: 23660394]
7. Bianchi MC, Tosetti M, Battini R, et al. Treatment monitoring of brain creatine deficiency syndromes: A $^{1}$H- and $^{31}$P-MR spectroscopy study. Am J Neuroradiol. 2007;28(3):548–554. [PubMed: 17353334]
8. Stockler S, Holzbach U, Hanefeld F, et al. Creatine deficiency in the brain: A new, treatable inborn error of metabolism. Pediatr Res. 1994;36(3):409–413. [PubMed: 7808840]
9. Ndika JDT, Johnston K, Barkovich JA, et al. Developmental progress and creatine restoration upon long-term creatine supplementation of a patient with arginine:glycine amidinotransferase deficiency. Mol Genet Metab. 2012;106(1):48–54. [PubMed: 22386973]
10. Schulze A, Hess T, Wevers R, et al. Creatine deficiency syndrome caused by guanidinoacetate methyltransferase deficiency: Diagnostic tools for a new inborn error of metabolism. J Pediatr. 1997;131(4):626–631. [PubMed: 9386672]
11. Cecil KM, Salomons GS, Ball WS, et al. Irreversible brain creatine deficiency with elevated serum and urine creatine: a creatine transporter defect? Ann Neurol. 2001;49(3):401–404. [PubMed: 11261517]
12. Salomons GS. van Dooren SJM, Verhoeven NM, et al. X-linked creatine-transporter gene (*SLC6A8*) defect: A new creatine deficiency syndrome. Am J Hum Genet. 2001;68:1497–1500. [PubMed: 11326334]
13. Mencarelli MA, Tassini M, Pollazzon M, et al. Creatine transporter defect diagnosed by proton NMR spectroscopy in males with intellectual disability. Am J Med Genet. Part A 2011;155(10):2446–2452.
14. Heussinger N, Saake M, Mennecke A, Dorr HG, Trollmann R. Variable white matter atrophy and intellectual development in a family with X-linked creatine transporter deficiency despite genotypic homogeneity. Pediatr Neurol. 2017;67:45–52. [PubMed: 28065824]
15. Xu S, Yang J, Li CQ, Zhu W, Shen J. Metabolic alterations in focally activated primary somatosensory cortex of alpha-chloralose-anesthetized rats measured by $^{1}$H MRS at 11.7 T. Neuroimage. 2005;28:401–409. [PubMed: 16182571]
16. Kitzenberg D, Colgan SP, Glover LE. Creatine kinase in ischemic and inflammatory disorders. Clin Transl Med. 2016;5:31–40. [PubMed: 27527620]
17. Vanhamme L, van den Boogaart A, van Huffel S. Improved method for accurate and efficient quantification of MRS data with use of prior knowledge. J Magn Reson. 1997;129(1):35–43. [PubMed: 9405214]
18. van der Kemp WJM, Klomp DWJ, Wijnen JP. $^{31}$P $T_2$s of phosphomonoesters, phosphodiesters, and inorganic phosphate in the human brain at 7T. Magn Reson Med. 2018;80:25–35.
19. Frahm J, Kruger G, Merboldt KD, Kleinschmidt A. Dynamic uncoupling and recoupling of perfusion and oxidative metabolism during focal brain activation in Man. Magn Reson Med. 1996;35(2):143–148. [PubMed: 8622575]
20. Kreis R. Quantitative localized $^{1}$H MR spectroscopy for clinical use. Prog Magn Reson Spectrosp. 1997;31(2/3):155–195.
21. Pouwels PJW, Brockmann K, Kruse B, et al. Regional age dependence of human brain metabolites from infancy to adulthood as detected by quantitative localized proton MRS. Pediatr Res. 1999;46(4):474–485. [PubMed: 10509371]
22. Rowland LM, Pradhan S, Korenic S, et al. Elevated brain lactate in schizophrenia: a 7T magnetic resonance spectroscopy study. Transl Psychiatry. 2016;6(11):e967 10.1038/tp.2016.239 [PubMed: 27898072]
23. Mekle R, Kuhn S, Pfeiffer H, Aydin S, Schubert F, Ittermann B. Detection of metabolite changes in response to varying visual stimulation paradigm using short-TE $^{1}$H MRS at 3T. NMR Biomed. 2017;30(2):e3672 10.1002/nbm.3672

24. Hubesch B, Sappey-Marinier D, Roth K, Meyerhoff DJ, Matson GB, Weiner MW. P-31 MR spectroscopy of normal human brain and brain tumors. Neurorad. 1990;174:401–409.
25. Hoang TQ, Bluml S, Dubowitz DJ, et al. Quantitative proton-decoupled $^{31}$P MRS and $^{1}$H MRS in the evaluation of Huntington's and Parkinson's diseases. Neurology. 1998;50(4):1033–1040. [PubMed: 9566391]
26. Bluml S. Seymour KJ, Ross BD. Developmental changes in choline- and ethanolamine-containing compounds measured with proton-decoupled $^{31}$P MRS in in vivo human brain. Magn Reson Med. 1999;42(4):643–654. [PubMed: 10502752]
27. Buchli R, Martin E, Boesiger P, Rumpel H. Developmental changes of phosphorus metabolite concentrations in the human brain: A $^{31}$P magnetic resonance spectroscopy study *in vivo*. Pediatr Res. 1994;35(4):431–435. [PubMed: 8047379]
28. Zhu XH, Du F, Zhang Y, Chen W. Cerebral phosphate metabolite profiles and their differentiation in human, cat and rat brains: a comparison study of in vivo $^{31}$P MRS at high fields. Proc Intl Soc Magn Reson Med. 2008;120.
29. Ren J, Sherry AD, Malloy CR. $^{31}$P-MRS of healthy human brain: ATP synthesis, metabolite concentrations, pH and $T_1$ relaxation times. NMR Biomed. 2015;28(11):1455–1462. [PubMed: 26404723]
30. Chen C, Stephenson MC, Peters A, Morris PG, Francis ST, Gowland PA. $^{31}$P magnetization transfer magnetic resonance spectroscopy: Assessing the activation induced change in cerebral ATP metabolic rates at 3 T. Magn Reson Med. 2018;79(1):22–30. [PubMed: 28303591]
31. de Graaf RA, De Feyter HM, Brown PB, Nixon TW, Rothman DL, Behar KL. Detection of cerebral $NAD^+$ in humans at 7T. Magn Reson Med. 2017;78(3):828–835. [PubMed: 27670385]
32. Kim SY, Cohen BM, Chen X, et al. Redox dysregulation in Schizophrenia revealed by in vivo $NAD^+$/NADH measurement. Schizophrenia Bulletin. 2017;43(1):197–204. [PubMed: 27665001]
33. Xin Lijing, Ipek O, Beaumont M, et al. Nutritional ketosis increases NAD+/NADH ratio in healthy human brain: an in vivo study by $^{31}$P-MRS. Front Nutr 2018;5:62 10.3389/fnut.2018.00062 [PubMed: 30050907]
34. Adeva-Andany MM, González-Lucán M, Donapetry-García C, Fernández-Fernández C, Ameneiros-Rodríguez E. Glycogen metabolism in humans. BBA Clin. 2016;5:85–100. [PubMed: 27051594]
35. Chance B, Eleff S, Leigh JS, Sokolow D, Sapega A. Mitochondrial regulation of phosphocreatine/inorganic phosphate ratios in exercising human muscle: A gated $^{31}$P NMR study. Proc Natl Acad Sci USA. 1981;78(11):6714–6718. [PubMed: 6947247]
36. Sappey-Marinier D, Calabrese G, Fein G, Hugg JW, Biggins C, Weiner MW. Effect of photic stimulation on human visual cortex lactate and phosphates using $^{1}$H and $^{31}$P magnetic resonance spectroscopy. J Cereb Blood Flow Metab. 1992;12(4):584–592. [PubMed: 1618937]
37. Adanyeguh IM, Rinaldi D, Henry PG, et al. Triheptanoin improves brain energy metabolism in patients with Huntington disease. Neurology. 2015;84(5):490–495. [PubMed: 25568297]
38. Shen J, Novotny EJ, Rothman DL. In vivo lactate and β-hydroxybutyrate editing using a pure-phase refocusing pulse train. Magn Reson Med. 1998;40(5):783–788. [PubMed: 9797163]
39. Prichard J, Rothman D, Novotny E, et al. Lactate rise detected by $^{1}$H NMR in human visual cortex during physiologic stimulation. Proc Natl Acad Sci USA. 1991;88(13):5829–5831. [PubMed: 2062861]
40. Brown AM, Tekkok SB, Ransom BR. Energy transfer from astrocytes to axons: the role of CNS glycogen. Neurochem Int. 2004;45(4):529–536. [PubMed: 15186919]
41. Cerdan S, Subramanian VH, Hilberman M, et al. $^{31}$P NMR detection of mobile dog brain phospholipids. Magn Reson Med. 1986;3(3):432–439. [PubMed: 3724422]
42. Cadoux-Hudson TA, Blackledge MJ, Rajagopalan B, Taylor DJ, Radda GK. Human primary brain tumour metabolism in vivo: a phosphorus magnetic resonance spectroscopy study. Br J Cancer. 1989;60(3):430–436. [PubMed: 2551360]
43. Pritchard NR, Kalra PA. Renal dysfunction accompanying oral creatine supplements. Lancet 1998;351(9111):1252–53. [PubMed: 9643752]

44. Garbati P, Adriano E, Salis A, et al. Effects of amide creatine derivatives in brain hippocampal slices, and their possible usefulness for curing creatine transporter deficiency. Neurochem Res. 2014;39(1):37–45. [PubMed: 24213972]

45. Giusti L, Molinaro A, Alessandrì MG, et al. Brain mitochondrial proteome alteration driven by creatine deficiency suggests novel therapeutic venues for creatine deficiency syndromes. Neuroscience. 2019;409:276–289. [PubMed: 31029731]

46. Leuner K, Kurz C, Guidetti G, Orgogozo JM, Müller WE. Improved mitochondrial function in brain aging and Alzheimer disease – the new mechanism of action of the old metabolic enhancer piracetam. Front Neurosci. 2010;4:44 10.3389/fnins.2010.00044

47. Sugiura Yuki, Honda Kurara, Kajimura Mayumi, Suematsu Makoto. Visualization and quantification of cerebral metabolic fluxes of glucose in awake mice. Proteomics 2014;14(7/8):829–838. [PubMed: 23970501]

48. Obel LF, Müller MS, Walls AB, Sickmann HM, Bak LK, Waagepetersen HS, Schousboe A. Brain glycogen—new perspectives on its metabolic function and regulation at the subcellular level, Front Neuroenerg. 2012;4:3 10.3389/fnene.2012.00003

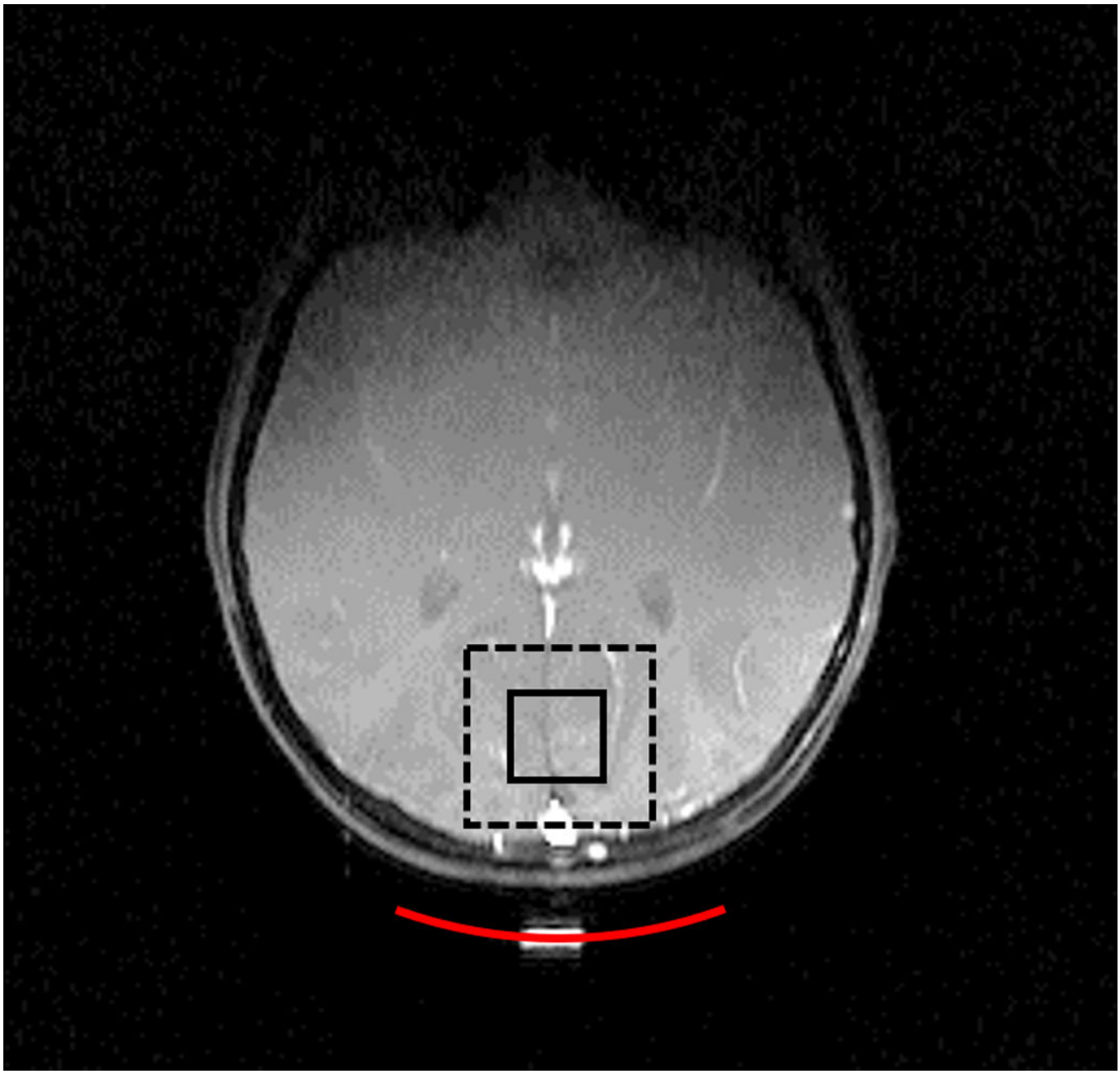

**Figure 1.**

Axial image of brain with the 4 × 4 × 4 $cm^3$ shim voxel (dashed box), and the 2 × 2 × 2 $cm^3$ proton MRS voxel (white box). The position of the $^{31}P$ surface coil was depieced by a red arc.

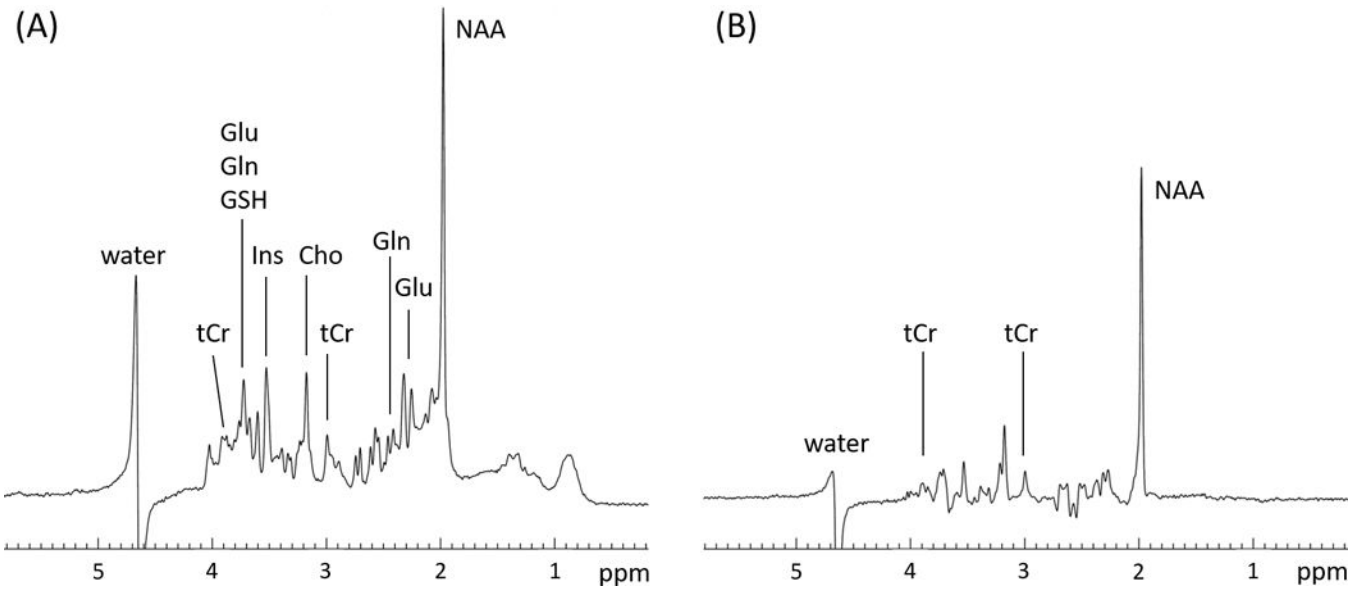


**Figure 2.**

Representative proton spectra obtained from a CTD patient. A, PRESS $^{1}$H spectrum of the CTD patient acquired at $T_E$ = 30 ms; and B, PRESS $^{1}$H spectrum at $T_E$ = 135 ms. The voxel of 2 × 2 × 2 cm$^3$ was placed in the occipital lobe. Repetition time ($T_R$) = 2 s.Number of averages (NA) = 128. Signal of total creatine was significantly reduced. There is no discernible lactate in the spectrum acquried at $T_E$ = 135 ms. Gln, glutamine; GSH, glutathione

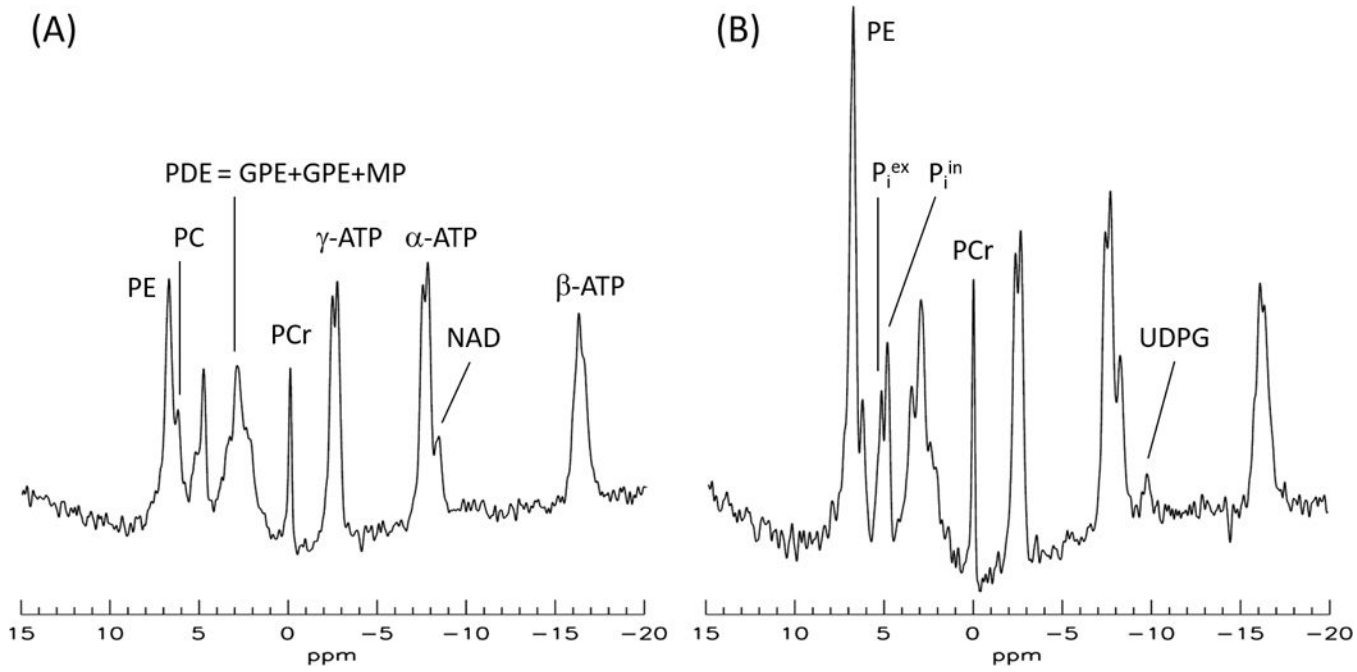


**Figure 3.**

Representative $^{31}$P spectra of CTD acquired at $T_R$ = 2 s and NA = 128 (A), and $T_R$ = 25 s and NA = 64 (B). PCr signal was substantially reduced. For the spectrum at $T_R$ = 25 s, most of the signals were substantially increased as compared with that at $T_R$ = 2 s. The UDPG $P_\beta$ signal, which is known to reside at −9.83 ppm was also detected.

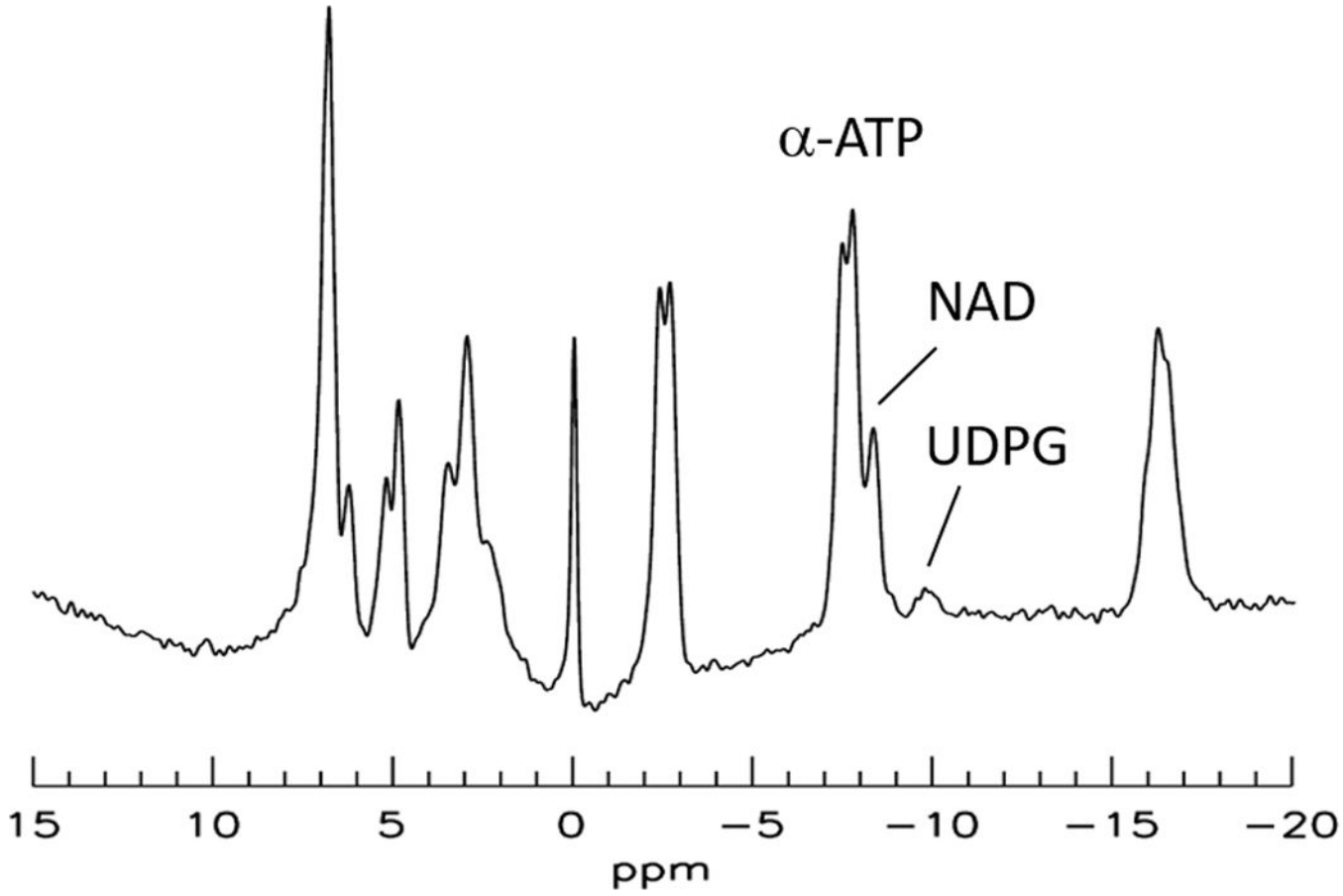


**Figure 4.**
Summed spectrum from seven patients with CTD ($T_R$ = 25 s).

**Table 1.**

Metabolite ratios of patients with CTD measured by $^{1}$H MRS.

| Metabolite ratios | Patients with CTD (n = 14) | | Healthy subject results from literature | |
|---|---|---|---|---|
| | Mean | SD | Range | References |
| tCr/NAA[a] | 0.12 | 0.02 | 0.65–0.81 | 19 – 23 |
| Glu/NAA[a] | 0.92 | 0.14 | 0.75–1.04 | 19 – 23 |
| Cho/NAA[a] | 0.10 | 0.01 | 0.08–0.13 | 19 – 23 |
| mI/NAA[a] | 0.51 | 0.05 | 0.40–0.57 | 19 – 23 |
| Lac/NAA[a] | 0.042 | 0.007 | 0.05–0.07 | 19, 22, 23 |
| Lac/NAA[b] | 0.025 | 0.014 | | |

[a] measured at $T_E$ = 30 ms

[b] measured at $T_E$ = 135 ms.

SD, standard deviation; tCr, total creatine; Lac, lactate.

**Table 2.**

Metabolite ratios of patients with CTD measured by $^{31}$P MRS

| Metabolite ratios | $T_R$ (s) | Patients with CTD | | Healthy subject results from literature | |
|---|---|---|---|---|---|
| | | n | Mean, SD | Range | References |
| PCr/γ-ATP | 2 | 14 | 0.22, 0.03 | 1.02–1.48 | 24 – 26[a] |
| | 25 | 7 | 0.26, 0.03 | 1.12–1.46 | 27 – 30[b] |
| $tP_i$/γ-ATP | 2 | 14 | 0.58, 0.07 | 0.36–0.52 | 24 – 26[a] |
| | 25 | 7 | 0.70, 0.13 | 0.35–0.54 | 27 – 30[b] |
| $tP_i$/PCr | 2 | 14 | 2.7, 0.5 | 0.35–0.36 | 24 – 26[a] |
| | 25 | 7 | 2.8, 0.4 | 0.26–0.4448 | 27 – 30[b] |
| NAD/γ-ATP | 2 | 14 | 0.15, 0.02 | | |
| | 25 | 7 | 0.25, 0.02 | 0.093–0.31 | 28 – 30[b] |
| UDPG/γ-ATP | 25 | 7 | 0.13, 0.04 | | |
| UDPG/NAD | 25 | 7 | 0.51, 0.16 | 0.28–0.88 | 30[b], 32[b], 28[b] 31[b] |

[a]Measurements with $T_R$ from 1.5 s to 2 s

[b]measurements with $T_R$ from 12 s to 30 s.